Supporting Information

$NiCo_2O_4$ with controllable oxygen vacancy concentration as high-efficient electrocatalyst for oxygen evolution reaction

Shangzhi Yao[a,b] , Haoshan Wei[a,b], Yong Zhang*[a,b], Xueru Zhang[c], Yan Wang[a,b], Jiaqin Liu[d], Hark Hoe Tan[e,f], Ting Xie[b], Yucheng Wu*[a,b]

[a] School of Materials Science and Engineering, Hefei University of Technology, Hefei 230009, Anhui, China.

[b]Key Laboratory of Advanced Functional Materials and Devices of Anhui Province, Hefei 230009, China

[c]Instrumental Analysis Center, Hefei University of Technology, Hefei 230009, China

[d]Institute of Industry & Equipment Technology, Hefei University of Technology, Hefei 230009, Anhui, China

[e]China International S&T Cooperation Base for Advanced Energy and Environmental Materials, Hefei 230009, Anhui, China

[f]Department of Electronic Materials Engineering, Research School of Physics and Engineering, The Australian National University, Canberra, ACT 2601, Australia

Email:*Yong Zhang : zhangyong.mse@hfut.edu.cn *Yucheng Wu:ycwu@hfut.edu.cn

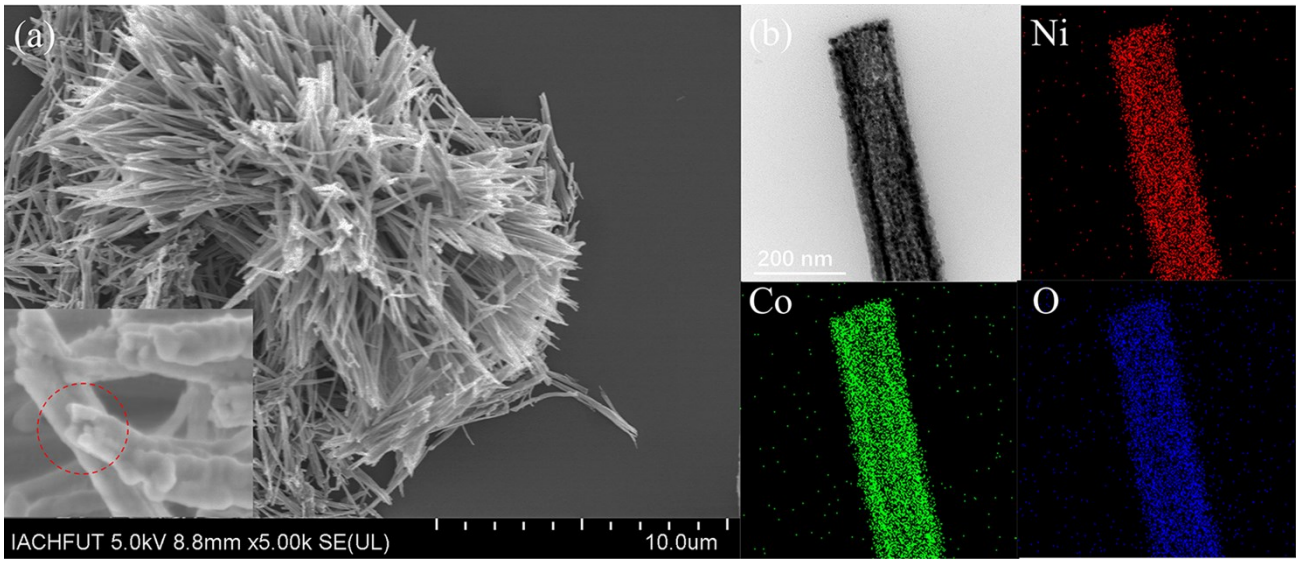

Figure S1. Field emission scanning electron microscope images (inset: magnified fracture images) and EDS mapping of $NiCo_2O_4$-OV-400.

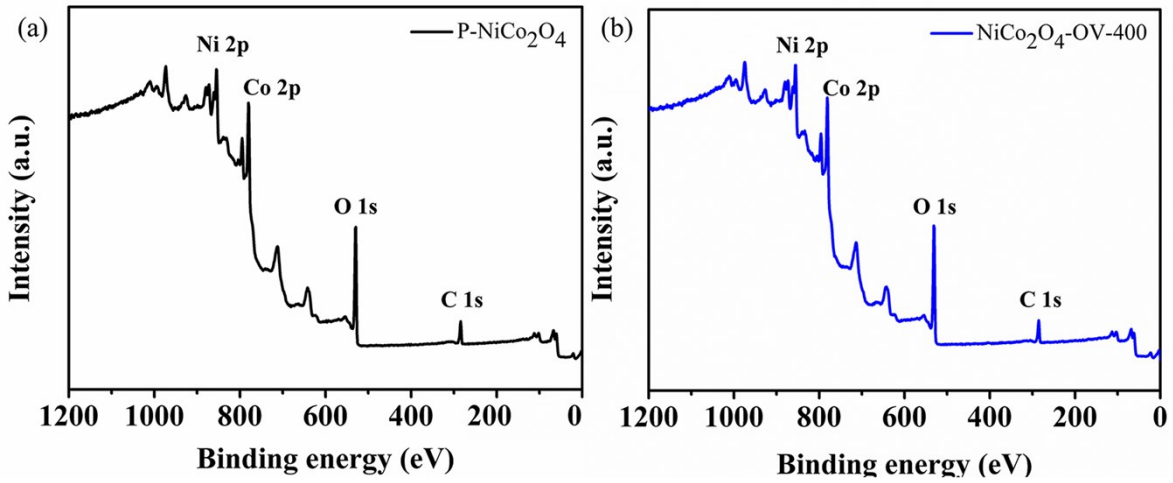

Figure S2. XPS survey of as-prepared (a) P-$NiCo_2O_4$ and (b) $NiCo_2O_4$-OV-400 samples.

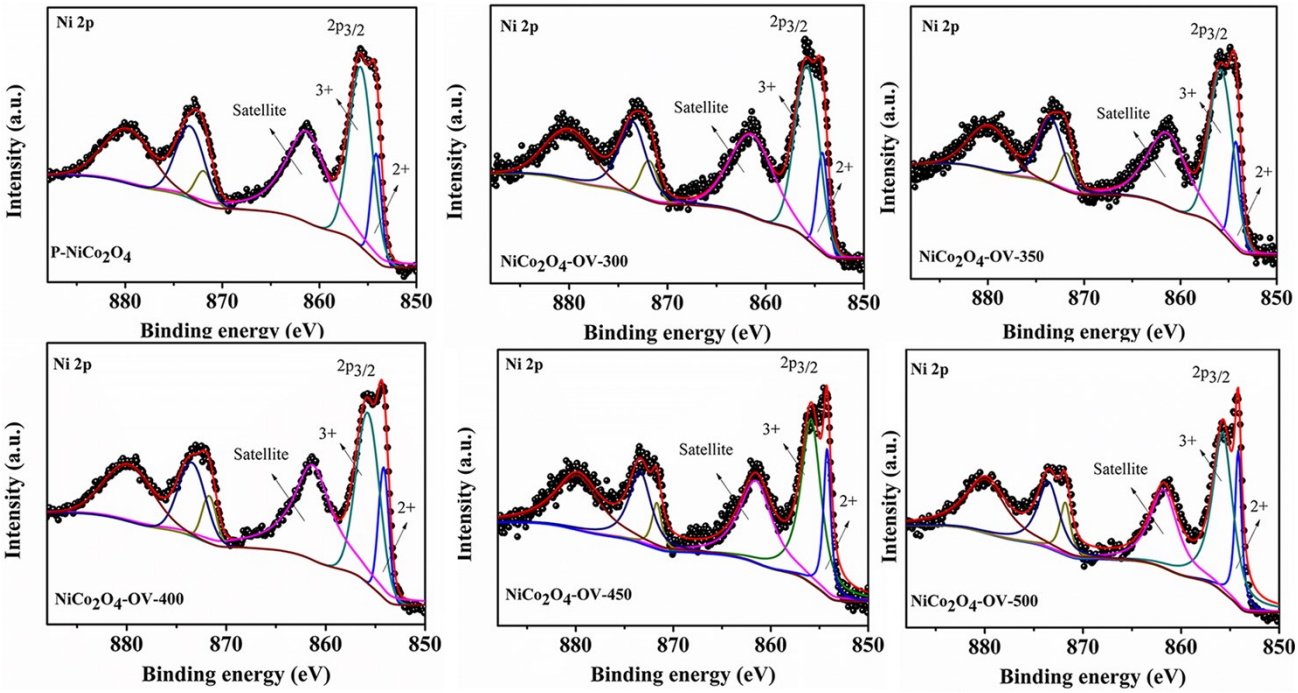

Figure S3. XPS spectra of Ni 2p in as-prepared $NiCo_2O_4$ nanobelts.

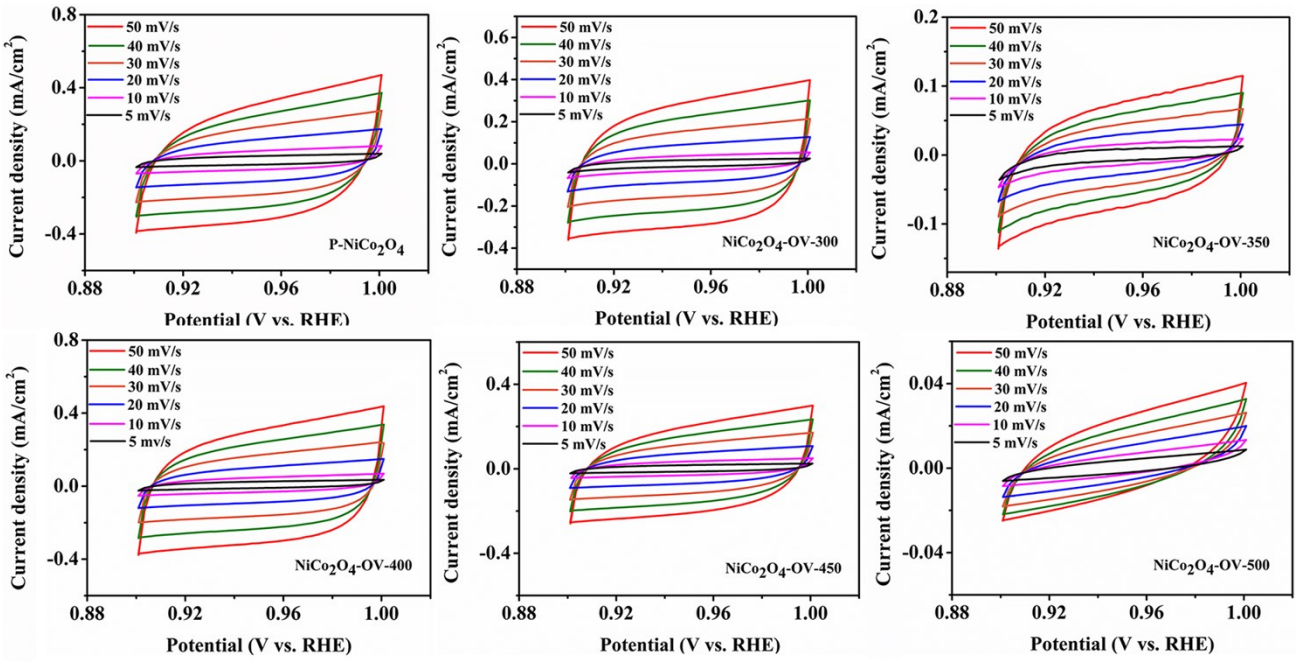

Figure S4. CVs of the double-layer capacitance measurement for the six different samples in 1 M KOH in the non-Faradaic region of 0.90-1.00 V vs. RHE with different scan rates, varying from 5 mV/s to 50 mV/s.

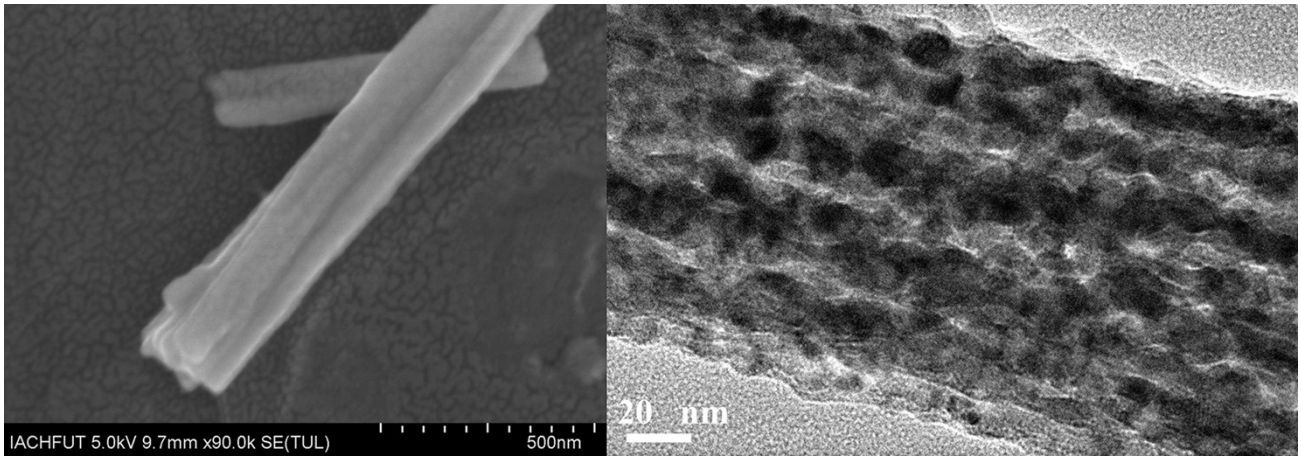

Figure S5. (a) SEM and (b) TEM of $NiCo_2O_4$-OV-400 after the long-time stability test (NCO-ST).

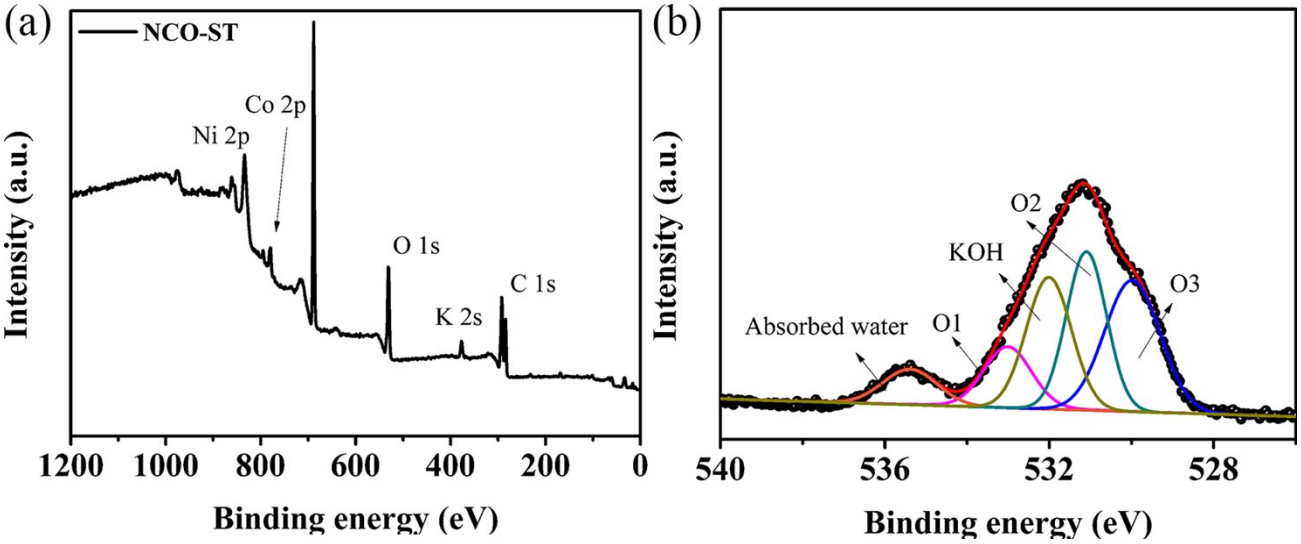

Figure S6. (a) XPS survey and (b) XPS spectrum of O 1s of NCO-ST.

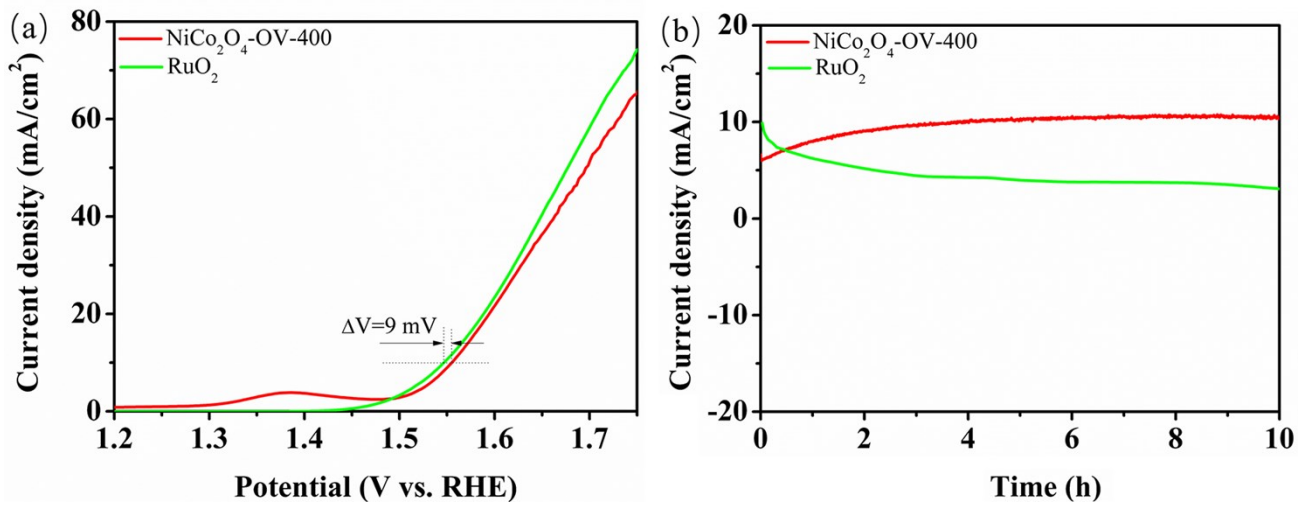

Figure S7. (a) The polarization of OER and (b) chronoamperometry curves of as-prepared $NiCo_2O_4$-

OV-400 and RuO_2 electrode in 1 M KOH. The chronoamperometry curves of $NiCo_2O_4$-OV-400 and RuO_2 for OER were tested at 1.55 V for 10 h.

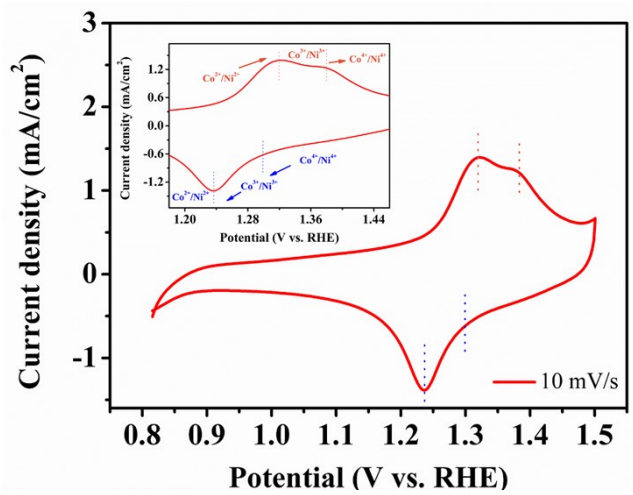

Figure S8. CV curve of $NiCo_2O_4$-OV-400 at a scan rate of 10 mV/s (Inset was the corresponding high magnification image).

Catalysts	Electrolyte	Substate	Overpotential (mV)	Tafel (mV/dec)	References
$NiCo_2O_4$-OV-400	1 M KOH	GC	325	71	This work
$NiCo_2O_4$	1 M KOH	GC	399	83	This work
HU-$NiCo_2O_4$	1 M NaOH	GC	419.3	51.3	33
P-Co_3O_4	1 M KOH	Ti Mesh	280	51.6	39
$NiCo_2O_4$(CH_3OH)	1 M KOH	GC	380	45.7	47
CoO_x-4h	1 M KOH	GC	306	65	48
NiCo-air	0.1 M KOH	GC	440	75	53
$NiCo_2O_4$-400°C	1 M KOH	FTO	375	54	64
Co/NCO/NF	0.1 M KOH	Ni foam	320	84	S1
$NiCo_2O_{4-\delta}$	0.1 M KOH	GC	390	——	S2
M-Co_3O_4	0.1 M KOH	GC	~370	89	S3

Table S1. A brief comparison of $NiCo_2O_4$-OV-400 nanobelts with other spinel oxides in the recent literature for OER.

References

S1. M. Yang, W. Lu, R. Jin, X.-C. Liu, S. Song and Y. Xing, ACS Sustainable Chem. Eng., 2019, 7, 12214-12221.

S2. I. Abidat, N. Bouchenafa-Saib, A. Habrioux, C. Comminges, C. Canaff, J. Rousseau, T. W. Napporn, D. Dambournet, O. Borkiewicz and K. B. Kokoh, J. Mater. Chem. A, 2015, 3, 17433-17444.

S3. H. Sun, Y. Zhao, K. Mølhave, M. Zhang and J. Zhang, *Nanoscale*, 2017, **9**, 14431-14441.